

Beta-delayed particle emission and collective rotations

K. Riisager¹, E.A.M. Jensen¹, A.S. Jensen¹

¹*Department of Physics and Astronomy, Aarhus University, DK-8000 Aarhus C, Denmark*

Beta-delayed proton emission in the lower half of the sd-shell will involve deformed nuclei. We derive the normalized matrix element connecting emission of one particle from an initial rotational nuclear state to another final rotating state, and we extract selection rules involving the K quantum number. The initial state is approximated as having a core identical to the final nuclear state. The formalism is then directly applicable to β^+ -delayed proton decays of even- Z , odd- N nuclei or β^- -delayed neutron decays of odd- Z , even N nuclei. These beta-decay results are compared to the outcomes of possible transfer reactions. As an example the beta-delayed proton emission of ^{21}Mg is considered, where new quantum numbers can be assigned to several states in ^{21}Na .

PACS numbers:

I. INTRODUCTION

This paper was motivated by a study of beta-delayed particle emission in the lower sd-shell, a region where nuclei are known to be well deformed. We shall focus mainly on the structure information that may arise from the particle emission process in the case of deformed nuclei that exhibit rotational behaviour. Much information can of course be extracted by populating the states in particle elastic scattering or transfer reactions, including detailed information on the composition of the wave-functions, see e.g. chapter 5.3a in [1], but the selection rules of the beta decay process will give a different feeding pattern, and focussing on the particle emission rather than state population can give complementary results. The beta-delayed particle process will give information on states placed above particle thresholds where emission of gamma-rays is often negligible.

We shall first derive general expressions for transition matrix elements, when the particle emitting initial state and the final state are similar rotations differing only by the extra emitted particle. They shall be derived based on the general formalism given in [2, 3]. The results are then applied to beta-delayed proton decays of ^{21}Mg . A more general discussion of the applicability of the results will also be given at the end of the paper. Before turning to the concrete formulation of the particle emission, we recall briefly some relevant aspects of the beta-decay process.

Beta-decay can give precise information on nuclear structure. The relevant interaction is extremely weak compared to the all-decisive, structure determining, strong interaction and the selection rules of the decay highlight a clean set of nuclear levels. As we move away from beta-stability, beta-delayed emission of particles like neutrons, protons or α -particles becomes more probable. These beta-delayed particles carry information on many aspects of the nuclear structure of the states in the decay cascade [4, 5].

The spin-isospin selection rules for allowed beta decay are as follows. For Fermi decays neither angular momentum J , nor isospin T , can change, for Gamow-Teller

decays the changes, ΔJ and ΔT , can be $0, \pm 1$ with no change in parity. All β^- decays (except that of the neutron and ^3H) will have $\Delta T = -1$, and the following emission of a particle will conserve isospin (and only reach final nuclei with higher T in the rare [6] β^- -p process). In light nuclei β^+ -delayed particle emission will mainly proceed in a similar way — the key difference is that Fermi decays to the isobaric analogue state (IAS) are now also energetically possible — and we shall mainly consider such systems.

Selection rules for beta transitions in strongly deformed nuclei are given in [1, 7]; out of the asymptotic single-particle Nilsson quantum numbers only Ω (the angular momentum projection on the intrinsic symmetry axis) may change by up to one unit for unhindered transitions, whereas at finite deformation allowed (but hindered, i.e. with some configuration mismatch) transitions may also take place. These results can of course also be derived with the methods employed in the next section, and will apply for the many-body quantum number K , the projection of the total angular momentum on the intrinsic symmetry axis. Results from charge-exchange reactions indicate [8] that the K -selection rule is most important for the region of interest here, where deformation parameters are large, $\delta \approx 0.4$.

We note that deformation in the beta-particle daughter nucleus for rotational states gives lower-than-usual excitation energies. This may increase the probability of beta-delayed particle emission to excited states, allowing richer structure information to be extracted.

The structure of the paper is as follows. In the next section the general result for particle emission between two deformed nuclei is derived. Section 3 treats the case of $K = 1/2$ and how results turn out in the particle-rotor model. Section 4 discusses our results in general, and section 5 outlines the connections to what can be obtained in transfer reactions. Section 6 applies the formalism to the decay of ^{21}Mg and extracts new structure information. Section 7 gives our summary and conclusions, and the appendices outline technical relations and definitions.

II. PROBLEM FORMULATION

We assume one rotational state in the initial (beta-populated) parent nucleus, ${}^{A_i}\text{XP}$, with quantum numbers J' , M' , and K' , where these quantum numbers describe, respectively, total angular momentum, its projection on the laboratory z -axis and on the intrinsic (symmetry) z -axis. This state emits a particle and populates a rotational state with quantum numbers J , M and K in the daughter nucleus, ${}^{A_f}\text{XD}$. The decay sequence is illustrated in the top part of Fig. 1.

A. Initial and final states

The wave function in the intrinsic body-fixed system is denoted $\Psi_{K'}(\{\mathbf{r}_i\})$, where \mathbf{r}_i stands for spin, isospin and space coordinate of nucleon $i \in [1, A_i]$ in this coordinate system. This initial rotational state is then [3]

$$\int d^3\vec{\omega}' \mathcal{D}_{M'K'}^{J'}(\vec{\omega}') |\Psi_{K'}(\{\mathcal{R}_{\vec{\omega}'}\mathbf{r}_i\})\rangle, \quad (1)$$

where $\mathcal{R}_{\vec{\omega}'}$ is the operator rotating the space and spin vector, \mathbf{r}_i , successively by the three Euler angles, $\vec{\omega}'$. Its matrix elements constitute the D -function, $\mathcal{D}_{M'K'}^{J'}(\vec{\omega}')$. The precise definitions are given in Appendix A together with a number of useful properties.

The structure in Eq.(1) expresses that the rotational state is described by a deformed wave function in the intrinsic body-fixed coordinate system. Integration over all angles weighted with the proper D -function subsequently restores the correct angular momentum and its projection on the laboratory coordinate system.

The final state consists of the emitted particle and another nuclear rotational state. We describe the emitted particle with coordinate, \mathbf{r}_p , as a plane wave with wave number, \mathbf{k}_p , multiplied by the spin function, χ_{Σ_p} . The particle wave function is then

$$\begin{aligned} \varphi_{\mathbf{k}_p}(\mathbf{r}_p) &= \chi_{\Sigma_p} \exp(i\mathbf{k}_p \cdot \mathbf{r}_p) \\ &= \chi_{\Sigma_p} 4\pi \sum_{l, m_l} i^l j_l(k_p r_p) Y_{l, m_l}(\hat{\mathbf{r}}_p) Y_{l, m_l}^*(\hat{\mathbf{k}}_p), \end{aligned} \quad (2)$$

where the $\hat{\cdot}$ denotes angles only. If the particle is charged, the plane wave can be replaced by an outgoing Coulomb wave function, or by a distorted wave function, if an optical potential is used.

The final state rotational wave function formally has the same structure as Eq.(1), that is

$$\int d^3\vec{\omega} \mathcal{D}_{MK}^J(\vec{\omega}) |\Psi_K(\{\mathcal{R}_{\vec{\omega}}\mathbf{r}_i\})\rangle, \quad (3)$$

where the quantum numbers have the same meaning as in Eq.(1), and the intrinsic wave function also has the same appearance, but referring to a smaller set of nucleons.

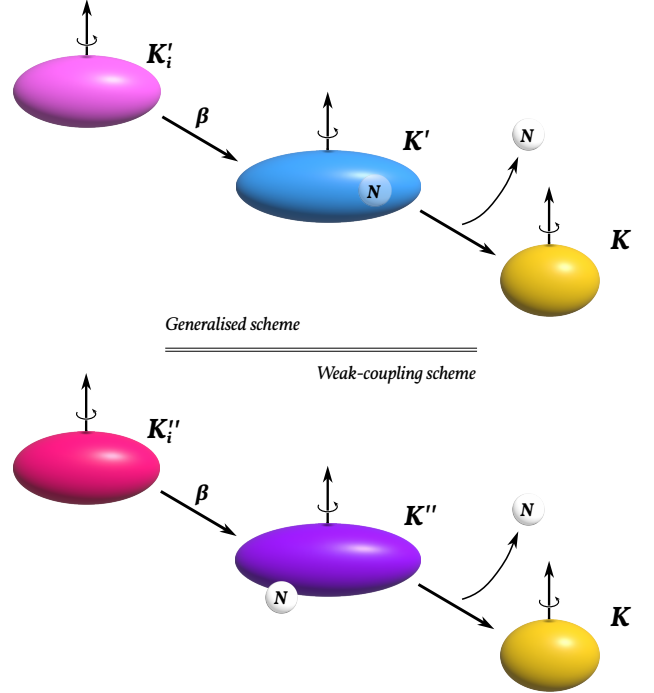


Figure 1: Schematic illustration of the beta-delayed particle emission involving rotational states. Top: In the general formulation the particle N is emitted from a rotating state with many-body quantum number K' that is populated in beta-decay. The final state has quantum number K . Bottom: In the weak-coupling scheme the state populated in beta-decay is a rotating state with quantum number K'' coupled in the laboratory system to the particle. The final state is the same.

B. Overlap matrix element

Formally, we describe the beta-delayed particle emission process through the matrix element between the beta-decaying state and the above final state with the beta decay operator in between. By inserting a complete set of states in the nucleus ${}^{A_i}\text{XP}$ we end up with a sum over beta matrix elements multiplied with different overlap matrix elements ME and shall focus on the latter in the following.

Using Eqs.(1), (2) and (3), the overlap matrix element, ME , between final and initial states is

$$\begin{aligned} ME &= 4\pi \sum_{l, m_l} (-i)^l Y_{l, m_l}(\hat{\mathbf{k}}_p) \int \int d^3\vec{\omega}' d^3\vec{\omega} \\ &\mathcal{D}_{MK}^{J*}(\vec{\omega}) \mathcal{D}_{M'K'}^{J'}(\vec{\omega}') \\ &\langle \Psi_K(\{\mathcal{R}_{\vec{\omega}}\mathbf{r}_i\}) | \chi_{\Sigma_p}^\dagger j_l^*(k_p r_p) Y_{l, m_l}^*(\hat{\mathbf{r}}_p) | \Psi_{K'}(\{\mathcal{R}_{\vec{\omega}'}\mathbf{r}_i\}) \rangle. \end{aligned} \quad (4)$$

To compute the overlap matrix element, we have to transform all coordinates to refer to the same frame. The particle coordinates of both spin and space, given in the laboratory system, are now rotated to the intrinsic system of the initial rotating nucleus. This is done by use of Eq.(A9) for each of the tensors, $\chi_{\Sigma_p}^\dagger$ and $Y_{l, m_l}^*(\hat{\mathbf{r}}_p)$, where

the same rotation angle then applies for both cases. Their respective orders are s and l , where $s = 1/2$ for nucleons and 0 for α -particles. The result is the same set of coordinates, named $\{\mathbf{r}'_i\}$, as seen in Eq.(A8).

The final state coordinates must also be transformed to the same intrinsic frame of the initial nucleus. This is done by use of the two successive rotations in Eq.(A6), also expressed in terms of the set $\{\mathbf{r}'_i\}$, but now rotated by $\mathcal{R}_{\vec{\omega}''}$. This leaves the final state D -function, with arguments ω , to be expressed in terms of ω'' and ω' , which is done in Eq.(A7). Altogether we can write the overlap in Eq.(4) as

$$ME = 4\pi \sum_{l,m_l} (-i)^l Y_{l,m_l}(\hat{\mathbf{k}}_p) \sum_{L,m'_l,\Sigma'_p} \int \int d^3\vec{\omega}'' d^3\vec{\omega}' \quad (5)$$

$$\mathcal{D}_{\Sigma_p\Sigma'_p}^{s*}(\vec{\omega}') \mathcal{D}_{m_l m'_l}^{l*}(\vec{\omega}') \mathcal{D}_{ML}^{J*}(\vec{\omega}') \mathcal{D}_{LK}^{J*}(\vec{\omega}'') \mathcal{D}_{M'K'}^{J'}(\vec{\omega}') \langle \Psi_K(\{\mathcal{R}_{\vec{\omega}''}\mathbf{r}'_i\}) | \chi_{\Sigma'_p}^\dagger j_l^*(k_p r'_p) Y_{l,m'_l}^*(\hat{\mathbf{r}}'_p) | \Psi_{K'}(\{\mathbf{r}'_i\}) \rangle .$$

Four of the D -functions in Eq.(5) have the same argument, $\vec{\omega}'$, which does not appear anywhere else, and consequently can be integrated out. Two of them are first combined into one by use of Eq.(A5), which naturally introduces the total angular momentum j of the emitted particle, and the integral over the remaining three D -functions are performed via Eq.(A10). The overlap in Eq.(5) then becomes

$$ME = \sum_{l,m_l,L,m'_l,\Sigma'_p,j} (-i)^l Y_{l,m_l}(\hat{\mathbf{k}}_p) \langle JMjm_l + \Sigma_p | J'M' \rangle \langle JLjm'_l + \Sigma'_p | J'K' \rangle \langle lm_l s \Sigma_p | jm_l + \Sigma_p \rangle \langle lm'_l s \Sigma'_p | jm'_l + \Sigma'_p \rangle \frac{32\pi^3}{2J'+1} \int d^3\vec{\omega} \mathcal{D}_{LK}^{J*}(\vec{\omega}) \langle \Psi_K(\{\mathcal{R}_{\vec{\omega}}\mathbf{r}_i\}) | \chi_{\Sigma'_p}^\dagger j_l^*(k_p r_p) Y_{l,m'_l}^*(\hat{\mathbf{r}}_p) | \Psi_{K'}(\{\mathbf{r}_i\}) \rangle . \quad (6)$$

One D -function is left with the argument $\vec{\omega}''$, now renamed to $\vec{\omega}$. If the parity of the initial and final nuclear states is the same (opposite), only even (odd) values of l are permitted. The Clebsch-Gordan coefficients imply that the summations are restricted from initial and final state quantum numbers, that is $m_l = M' - M - \Sigma_p$, $m'_l = K' - K - \Sigma'_p$, where $\Sigma'_p = \pm 1/2$ and furthermore $j = l \pm 1/2$ for nucleon emission, and $\Sigma'_p = 0$, $j = l$ for alpha particle emission.

C. Normalization

Before we attempt further reduction of the overlap in Eq.(6), we find the normalization factors N_i and N_f for the initial and final rotational wave functions, respectively. In other words, we must calculate

$$N_f = \int d^3\vec{\omega} \mathcal{D}_{MK}^{J*}(\vec{\omega}) \int d^3\vec{\omega}' \mathcal{D}_{MK}^J(\vec{\omega}') \langle \Psi_K(\{\mathcal{R}_{\vec{\omega}}\mathbf{r}_i\}) | \Psi_{K'}(\{\mathcal{R}_{\vec{\omega}'}\mathbf{r}_i\}) \rangle , \quad (7)$$

which can be reduced by the same technique as used for the overlap in Eq.(6). We then easily get

$$N_f = \frac{8\pi^2}{2J+1} \int d^3\vec{\omega} \mathcal{D}_{KK}^{J*}(\vec{\omega}) \langle \Psi_K(\{\mathcal{R}_{\vec{\omega}}\mathbf{r}_i\}) | \Psi_K(\{\mathbf{r}_i\}) \rangle , \quad (8)$$

and N_i follows in complete analogy, related to the other rotational wave function, where the nucleons belong to the initial state and the quantum numbers are instead J' , M' and K' .

Let us assume that the intrinsic states are strongly deformed. Then the overlaps in the central pieces of the matrix elements in Eqs.(6) and (7) must in the general case be very small unless the rotation angle, θ , is close to zero [3], that is

$$\langle \Psi_K(\{\mathcal{R}_{\vec{\omega}}\mathbf{r}_i\}) | OP | \Psi_{K'}(\{\mathbf{r}_i\}) \rangle \simeq \langle OP \rangle \exp(iK(\psi + \phi) - \theta^2/\theta_0^2) . \quad (9)$$

(This is discussed further in appendix B.) The average of the operator, $\langle OP \rangle$, is either 1 from Eq.(7) or the function of the emitted particle coordinates in Eq.(6). Using the value of the D -function for $\theta = 0$ as

$$\mathcal{D}_{LK}^{J*}(\phi, \theta = 0, \psi) = \delta_{LK} \exp(-iK(\psi + \phi)) , \quad (10)$$

we have for the normalizations

$$N_f \simeq \frac{8\pi^2(2\pi)^2\theta_0^2}{2(2J+1)} , \quad N_i \simeq \frac{8\pi^2(2\pi)^2\theta_0^2}{2(2J'+1)} . \quad (11)$$

D. Normalized overlap

In analogy to the above we find for the integral in Eq.(6)

$$\int d^3\vec{\omega} \mathcal{D}_{LK}^{J*}(\vec{\omega}) \langle \Psi_K(\{\mathcal{R}_{\vec{\omega}}\mathbf{r}_i\}) | \chi_{\Sigma'_p}^\dagger j_l^*(k_p r_p) Y_{l,m'_l}^*(\hat{\mathbf{r}}_p) | \Psi_{K'}(\{\mathbf{r}_i\}) \rangle \simeq \delta_{LK} \frac{1}{2} (2\pi)^2 \theta_0^2 \int d^3\mathbf{r}_p \chi_{\Sigma'_p}^\dagger j_l^*(k_p r_p) Y_{l,m'_l}^*(\hat{\mathbf{r}}_p) \varphi_{K'}(\mathbf{r}_p) , \quad (12)$$

where we assume that most of the nucleons in both initial and final states are in the same rotating state and the initial wave function for the emitted particle in the intrinsic frame of the initial system is $\varphi_{K'}(\mathbf{r}_p)$. (It is discussed in more detail in Appendix B.)

The overlap matrix element from Eq.(6) with the normalisations in Eq.(11) and the reduction in Eq.(12), finally gives

$$\frac{ME}{\sqrt{N_i N_f}} = 4\pi \sqrt{\frac{2J+1}{2J'+1}} \sum_{j,l,m_l,m'_l,\Sigma'_p} (-i)^l Y_{l,m_l}(\hat{\mathbf{k}}_p) \langle JMjm_l + \Sigma_p | J'M' \rangle \langle JKjm'_l + \Sigma'_p | J'K' \rangle \langle lm_l s \Sigma_p | jm_l + \Sigma_p \rangle \langle lm'_l s \Sigma'_p | jm'_l + \Sigma'_p \rangle \int d^3\mathbf{r}_p \chi_{\Sigma'_p}^\dagger j_l^*(k_p r_p) Y_{l,m'_l}^*(\hat{\mathbf{r}}_p) \varphi_{K'}(\mathbf{r}_p) . \quad (13)$$

Out of the four Clebsch-Gordan coefficients, the first and third ensure angular momentum conservation in the laboratory system, the second and fourth the conservation in the intrinsic system. The selection rule involving the K quantum number is specific to the deformed nuclei.

The emission rate of the particle is now proportional to the amplitude in Eq.(13) squared, summed over final states and averaged over initial states, i.e.

$$\frac{1}{2J'+1} \sum_{M,M'} \frac{|ME|^2}{N_i N_f} \quad (14)$$

Furthermore, one must sum or integrate over unobserved quantities, e.g. Σ_p and $\hat{\mathbf{k}}_p$.

III. THE CASE OF A $K = 1/2$ SYSTEM

The spectra of $K = 1/2$ bands in rotating nuclei do not show the usual $J(J+1)$ energy sequence. Instead the energies fluctuate up and down more like a $K = 1/2$ nucleon (we do not treat alpha particle emission in this section) that is coupled to a rotating zero angular momentum core [1, 3]. To test whether particle emission can be expressed in this framework, we derive the transition matrix element with the explicit rotator-coupling assumption, and afterwards compare to the general expression for the transition from a $K = 1/2$ initial structure.

A. Particle-rotor coupling

In the particle-rotor framework the final state remains the same, i.e. the product of Eqs.(2) and (3), whereas the initial state now is the coupling between a $j = 1/2$ nucleon with wave function in the laboratory coordinate system (i.e. the weak coupling limit [3]; we separate out the spin, angular and radial wave functions), and the rotating core with quantum numbers $J''M''K''$, see also the bottom part of Fig. 1:

$$\sum_{M'',m''_j,m''_l,\Sigma''} \langle J''M'' \frac{1}{2}m''_j | J' M' \rangle \langle l''m''_l \frac{1}{2}\Sigma'' | \frac{1}{2}m''_j \rangle Y_{l'',m''_l}(\hat{\mathbf{r}}_p) \chi_{\Sigma''} \varphi_{1/2}(r_p) \int d^3\vec{\omega}' \mathcal{D}_{M''K''}^{J''}(\vec{\omega}') |\Psi_{K''}(\{\mathcal{R}_{\vec{\omega}'}\mathbf{r}_i\})\rangle. \quad (15)$$

To compute the overlap matrix element, we use Eqs.(2), (3) and (15).

$$ME = 4\pi \sum_{l,m_l,M'',m''_j} (-i)^l Y_{l,m_l}(\hat{\mathbf{k}}_p) \langle J''M'' \frac{1}{2}m''_j | J' M' \rangle \langle lm_l \frac{1}{2}\Sigma_p | \frac{1}{2}m''_j \rangle \int \int d^3\vec{\omega}' d^3\vec{\omega} \mathcal{D}_{MK}^{J*}(\vec{\omega}) \mathcal{D}_{M''K''}^{J''}(\vec{\omega}') (16) \langle \Psi_K(\{\mathcal{R}_{\vec{\omega}}\mathbf{r}_i\}) | \varphi_{1/2}(r_p) j_l^*(k_p r_p) | \Psi_{K''}(\{\mathcal{R}_{\vec{\omega}'}\mathbf{r}_i\}) \rangle,$$

where we combined the spin and orbital wave functions, $\chi_{\Sigma''}$ and χ_{Σ_p} , and the orbital, Y_{l'',m''_l} and Y_{l,m_l} in initial and final states to give the δ -functions, $\delta_{\Sigma_p,\Sigma''}$, $\delta_{l,l''}$ and δ_{m_l,m''_l} . We continue to reformulate the integrations in Eq.(16) as was done above in going from Eq.(4) to Eq.(5). The nucleon's spin and orbital wave functions disappear, and we get the similar, but simpler expression with only three D -functions

$$ME = \sum_{l,m_l,L,M'',m''_j} 4\pi (-i)^l Y_{l,m_l}(\hat{\mathbf{k}}_p) \langle J''M'' \frac{1}{2}m''_j | J' M' \rangle \langle lm_l \frac{1}{2}\Sigma_p | \frac{1}{2}m''_j \rangle \int \int d^3\vec{\omega}' d^3\vec{\omega} \mathcal{D}_{ML}^{J*}(\vec{\omega}') \mathcal{D}_{LK}^{J*}(\vec{\omega}) \mathcal{D}_{M''K''}^{J''}(\vec{\omega}') \langle \Psi_K(\{\mathcal{R}_{\vec{\omega}'}\mathbf{r}_i\}) | j_l^*(k_p r_p) \varphi_{1/2}(r_p) | \Psi_{K''}(\{\mathbf{r}_i\}) \rangle. \quad (17)$$

The two D -functions with the same argument, $\vec{\omega}'$, are integrated to give the δ -functions, $\delta_{J,J''}$, $\delta_{M,M''}$ and $\delta_{L,K''}$, that is

$$ME = \sum_{l,m_l,m''_j} 4\pi (-i)^l Y_{l,m_l}(\hat{\mathbf{k}}_p) \langle JM \frac{1}{2}m''_j | J' M' \rangle \langle lm_l \frac{1}{2}\Sigma_p | \frac{1}{2}m''_j \rangle \frac{8\pi^2}{2J+1} \int d^3\vec{\omega} \mathcal{D}_{K''K}^{J*}(\vec{\omega}) \langle \Psi_K(\{\mathcal{R}_{\vec{\omega}}\mathbf{r}_i\}) | \Psi_{K''}(\{\mathbf{r}_i\}) \rangle \int d^3\mathbf{r}_p j_l^*(k_p r_p) \varphi_{1/2}(r_p). \quad (18)$$

Again, one D -function remains with the argument $\vec{\omega}'$, now renamed to $\vec{\omega}$. The assumptions of strong deformation and of identical initial and final state rotating cores, finally gives

$$\frac{ME}{\sqrt{N_i N_f}} = 4\pi \sum_{l,m_l,m''_j} (-i)^l Y_{l,m_l}(\hat{\mathbf{k}}_p) \langle JM \frac{1}{2}m''_j | J' M' \rangle \langle lm_l \frac{1}{2}\Sigma_p | \frac{1}{2}m''_j \rangle \int d^3\mathbf{r}_p j_l^*(k_p r_p) \varphi_{1/2}(r_p). \quad (19)$$

This derivation explicitly highlights the assumption that the rotating cores are identical before and after the nucleon emission. Depending on whether there is a change or not in parity between the initial and final states, the l -values will be odd or even; this implies that $l = 0$ or $l = 1$ when the nucleon has total angular momentum of $j = 1/2$. Then Eq.(19) simplifies for $l = 0$ to

$$\frac{ME}{\sqrt{N_i N_f}} = \sqrt{4\pi} \langle JM \frac{1}{2}\Sigma_p | J' M' \rangle \int d^3\mathbf{r}_p j_0^*(k_p r_p) \varphi_{1/2}(r_p). \quad (20)$$

For $l = 1$ we are again left with only one term, that is

$$\frac{ME}{\sqrt{N_i N_f}} = -4\pi i Y_{1,m_l}(\hat{\mathbf{k}}_p) \langle JM \frac{1}{2}m''_j | J' M' \rangle$$

$$\langle 1m_l \frac{1}{2} \Sigma_p | \frac{1}{2} m_j'' \rangle \int d^3 \mathbf{r}_p j_1^*(k_p r_p) \varphi_{1/2}(r_p), \quad (21)$$

since $m_j'' = M' - M$ and $m_l = M' - M - \Sigma_p$. If desired, the Clebsch-Gordan coefficients can be explicitly inserted, where we get

$$\langle 1m_l \frac{1}{2} \Sigma_p | \frac{1}{2} m_j'' \rangle = (-1)^{1/2 + \Sigma_p} \sqrt{\frac{1 - 2\Sigma_p m_l}{3}} \quad (22)$$

with $m_l = M' - M - \Sigma_p$.

B. Special particle-rotor model results

Eq.(20) becomes simpler for transitions to the ground state, where $J = K = M = 0$ and the parity is even, in which case we get $J' = 1/2$, $M' = \Sigma_p = \pm 1/2$, and the expression:

$$\frac{ME}{\sqrt{N_i N_f}} = \sqrt{4\pi} \int d^3 \mathbf{r}_p j_0^*(k_p r_p) \varphi_{1/2}(r_p). \quad (23)$$

This means that only $\frac{1}{2}^+$ states can decay to the ground state via s -wave emission.

Whereas in the general case the emitted particle is described in the intrinsic system of the initial nucleus, it is in the weak coupling limit of the particle-rotor model described in the laboratory system. It is then of interest to see whether the final results are consistent.

The general formula in Eq.(13) will in the case of $K' = 1/2$ and $l = 0$ simplify: As $s = 1/2$ we have $j = 1/2$, and two of the Clebsch-Gordan coefficients are unity, so

$$\begin{aligned} \frac{ME}{\sqrt{N_i N_f}} &= \sqrt{4\pi} \sqrt{\frac{2J+1}{2J'+1}} \sum_{\Sigma_p'} \langle JM \frac{1}{2} \Sigma_p | J' M' \rangle \langle JK \frac{1}{2} \Sigma_p' | J' K' \rangle \\ &\int d^3 \mathbf{r}_p \chi_{\Sigma_p'}^\dagger j_0^*(k_p r_p) Y_{0,0}^*(\hat{\mathbf{r}}_p) \varphi_{K'}(\mathbf{r}_p). \end{aligned} \quad (24)$$

The wavefunction $\varphi_{K'}(\mathbf{r}_p)$ has a radial part, an angular part, which must have $l = 0$ to make the integral nonvanishing, and a spin part. A closer inspection shows that $\varphi_{K'}(\mathbf{r}_p)$ will have two terms (with quantum numbers $\pm K'$). This more general structure is discussed in Appendix B where the equivalence of the two formulations is shown explicitly for $K = 0$.

IV. GENERAL RESULTS

This section discusses specific results of the general formalism for emission of nucleons and α particles as well as the selection rules in J and K .

A. Selection rules

The Clebsch-Gordan coefficients in Eq.(13) imply that

$$\vec{J} + \vec{j} = \vec{J}', \quad |M - M'| \leq j, \quad |K - K'| \leq j, \quad (25)$$

corresponding to the conservation of angular momentum and that the difference in M and K values in the initial and final nucleus cannot differ by more than $j = l \pm s$. The interesting selection rule comes from the last term involving K , since all members of a rotational band will have the same value of K , but increasing values of J (and M). A difference in K -values can therefore enforce a higher value of j (and thereby of l) than allowed by angular momentum conservation alone. As a concrete example, only a $K' = 1/2$ band can emit s -wave nucleons to a $K = 0$ band.

For states that are band heads the J and K quantum numbers are the same (except possibly for K or $K' = 1/2$ bands) in which case there are no extra restrictions from the K -selection rule, but emission from (or to) levels higher in a band may be affected by it.

B. Emission of protons or neutrons

Nucleons have $s = 1/2$, so that given a value of l there are two possible j -values. However, due to parity conservation, given a value of j only one of the two orbital angular momentum values, $l = j \pm 1/2$, is permitted.

The probability of particle emission is given in Eq.(13) and depends (as usual) partly on the overlap matrix element, partly on the penetrability factor that is related to the square of the Bessel function (or Coulomb wave function for charged emitted particles), cf. chapters 7.4.1 and 10.2 in [9].

The first special case of interest is emission of nucleons to the ground state of an even-even nucleus. Since $J = M = K = 0$ this reduces Eq.(13) significantly, as $j = J'$, $m_l + \Sigma_p = M'$ and $m_l' + \Sigma_p' = K'$. The total expression reduces to

$$\begin{aligned} \frac{ME}{\sqrt{N_i N_f}} &= 4\pi \sqrt{\frac{1}{2J'+1}} \sum_{l, \Sigma_p'} (-i)^l Y_{l, m_l}(\hat{\mathbf{k}}_p) \\ &\langle l m_l \frac{1}{2} \Sigma_p | J' M' \rangle \langle l m_l' \frac{1}{2} \Sigma_p' | J' K' \rangle \\ &\int d^3 \mathbf{r}_p \chi_{\Sigma_p'}^\dagger j_l^*(k_p r_p) Y_{l, m_l'}^*(\hat{\mathbf{r}}_p) \varphi_{K'}(\mathbf{r}_p), \end{aligned} \quad (26)$$

The quantum numbers, M' and K' , have given values characterizing the initial state. The spin-projection, $\Sigma_p = \pm 1/2$, is in principle an observable in the final state characterizing the nucleon, which implies that $m_l = M' - \Sigma_p$. In contrast, the spin projection, Σ_p' , of the nucleon in the initial state, $\Sigma_p' = \pm 1/2$, is still a summation index, which however implies $m_l' = K' - \Sigma_p'$.

As discussed in detail in the next section this expression is very similar to the one of transfer reactions on an

even-even nucleus [10]. Emission to higher states in the ground state band gives a more complex expression.

The second special case is that of emission of an $l = 0$ nucleon independent of what final state is reached. Clearly we have $m_l = m'_l = 0$ and $j = s = 1/2$. The simpler expression becomes

$$\frac{ME}{\sqrt{N_i N_f}} = \sqrt{\frac{2J+1}{2J'+1}} \sum_{\Sigma'_p} \langle JM \frac{1}{2} \Sigma_p | J' M' \rangle$$

$$\langle JK \frac{1}{2} \Sigma'_p | J' K' \rangle \int d^3 \mathbf{r}_p \chi_{\Sigma'_p, J'_0}^\dagger(k_p r_p) \varphi_{K'}(\mathbf{r}_p). \quad (27)$$

For emission to a $K = 0$ band the sum reduces to the term with $\Sigma'_p = K'$ and we recover the previous result that only a $K' = 1/2$ band can emit angular momentum zero protons to a $K = 0$ band.

C. Emission of α -particles

For α -particles $s = 0$ and $j = l$. Inserting this in Eq.(13) gives a significant simplification, i.e.

$$\frac{ME}{\sqrt{N_i N_f}} = 4\pi \sqrt{\frac{2J+1}{2J'+1}} \sum_{l, m_l, m'_l} (-i)^l Y_{l, m_l}(\hat{\mathbf{k}}_p)$$

$$\langle JM l m_l | J' M' \rangle \langle JK l m'_l | J' K' \rangle$$

$$\int d^3 \mathbf{r}_p \mathcal{J}_l^*(k_p r_p) Y_{l, m'_l}^*(\hat{\mathbf{r}}_p) \varphi_{K'}(\mathbf{r}_p). \quad (28)$$

Emission of s-wave α -particles must take place to states with exactly the same J , M and K as the original state and the normalized matrix element reduces to the following overlap integral

$$\frac{ME}{\sqrt{N_i N_f}} = \int d^3 \mathbf{r}_p \mathcal{J}_0^*(k_p r_p) \varphi_{K'}(\mathbf{r}_p). \quad (29)$$

V. RELATION TO TRANSFER REACTIONS

We have so far mainly discussed the particle emission process that can follow a beta-decay, see left hand side of Figure 2. As shown above, structure information for the emitting state can be derived from the decay pattern of the level. If the preceding beta particle is also detected, one can (provided the angular momenta of the participating states and the emitted particle is $1\hbar$ or larger) derive further constraints from the angular distribution between the beta particle and the emitted particle. There is also information from the beta decay selection rules (as mentioned in the introduction).

It may be enlightening to compare this to the information traditionally extracted from single-particle transfer reactions, see right hand side of Figure 2. A particle is transferred from a projectile to the target (with spin J) populating a level with spin J' , i.e. the reverse reaction

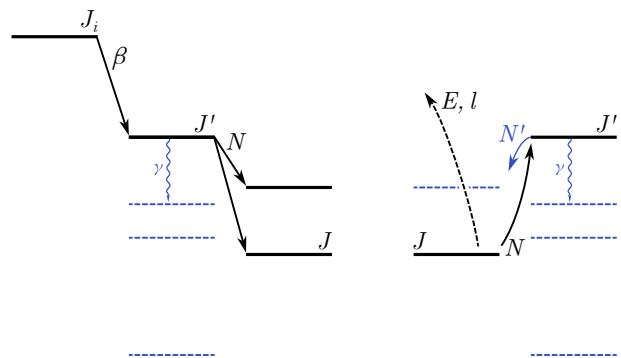


Figure 2: Left: Beta-delayed particle emission where the particle N is emitted from a level with spin J' to a level with spin J . Observables can be the energy and direction of the particle as well as the beta particle. Right: Transfer reaction from a level with spin J to a level with spin J' . Typical observables are the energy and angular distribution of the outgoing projectile-like fragment.

to the particle emission. Observation of the energy and angular distribution of the projectile fragment allow deduction of the excitation energy of the level and the angular momentum of the transferred particle. Note that levels both above and below the particle threshold in the final nucleus may be populated, but that only transitions from the ground state of the initial nucleus are probed. (If the experimental set-up allows, the decay of the level can of course also be recorded, in which case the formalism presented in this paper applies.)

Transfer reactions are often used to extract spectroscopic factors for single-particle configurations. The many-body matrix element in our Eq.(6) is closely related to the overlap functions that are used to define the spectroscopic factors, cf. chapter 5.3 in [9]. If we do not make the assumption in section II.D that the wave function of the level is completely described as a single particle outside the final state, we see that population of the level and the decay of it reveals the same physics information (as is to be expected).

The selection rule in Eq.(13) involving the K quantum number is specific to the deformed nuclei; a similar term occurs for transfer reactions that involve deformed nuclei, see e.g. section 4 in [10] and references therein. In the integral in Eq.(13) the spin and angular momentum parts of the wave function of the outgoing particle will select the parts of $\varphi_{K'}(\mathbf{r}_p)$ with the corresponding angular momentum; this is again similar to the overlap occurring for transfer reactions and gives rise to what is often named [1, 10] a “fingerprint” signal for the structure of the state. For transfer reactions this has been used to probe the structural details of Nilsson model states by populating different excited states in a rotational band. As the example in the next section shows, we can extract structure information for each state that emits particles to several final states and may possibly extract more detailed information through comparisons with theoretical

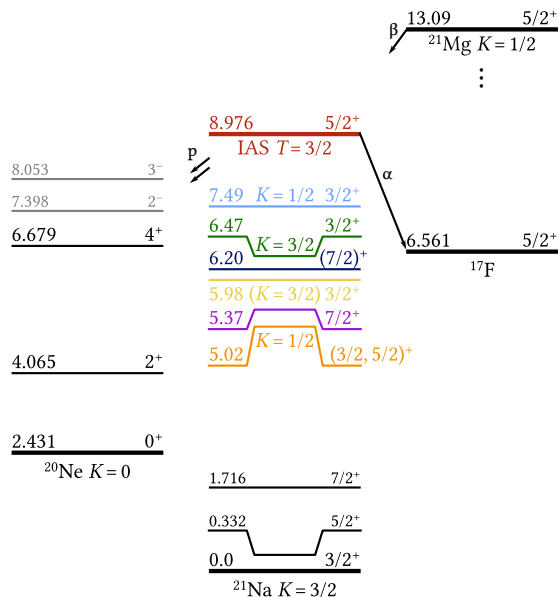


Figure 3: A sketch of some of the levels that occur in the beta-delayed proton decay of ^{21}Mg [14]. Several of the levels in ^{21}Na that are mentioned in the text are displayed with the colour coding being the same as in Figure 4.

structure calculations.

VI. THE DECAY OF ^{21}Mg

The practical use of the results will be illustrated with the decay of ^{21}Mg , where many aspects of the use of the formalism can be seen in a somewhat simple setting, since much of the structure of nuclei in the lower sd-shell can be discussed in terms of s-wave and d-wave nucleons, only. A brief overview of other possible cases is given in the last subsection.

The ground state of ^{21}Mg with one neutron in the Nilsson orbital $[220]1/2^+$ (the single-particle quantum numbers are $[Nn_z\Lambda]\Omega^P$) has spin-parity $5/2^+$ and is expected to be member of a $K = 1/2$ band with large positive decoupling parameter, as its mirror nucleus ^{21}F [1, 11] (see also [12, 13] for independent structure calculations). The isospin is $3/2$ and the same quantum numbers apply for the Isobaric Analogue State (IAS) at 8.97 MeV excitation energy in ^{21}Na , see Figure 3.

Allowed beta-decay of ^{21}Mg populates several excited states in ^{21}Na with $J' = 3/2, 5/2, 7/2$, positive parity and $K' = 1/2, 3/2$; those above 3.5 MeV excitation energy decay mainly by emitting protons to states in ^{20}Ne , at first only to the ground state but above 5 MeV excitation energy also to excited states. Most states fed in ^{20}Ne belong to the ground state rotational band of $K = 0$ and $J = 0, 2, 4$ with positive parity. A recent paper [14] gives an overview of the current experimental knowledge.

The general formalism given above will be used to set

restrictions on the quantum numbers of the observed levels and thereby expand the current knowledge on the rotational bands in ^{21}Na (see [1, 15] for established structure at lower excitation energy). Eq.(13) gives two general restrictions, the first arises from the Clebsch-Gordan coefficients (the selection rules) that imply that states with $K' = 1/2$ may emit both s-wave and d-wave protons, whereas $K' = 3/2$ may only emit d-wave protons.

The second restriction comes from consideration of the wave functions in the integral in Eq.(13). The internal single-particle wave function, $\varphi_{K'}(\mathbf{r}_p)$, mainly contains s- and d-waves (we are in the sd-shell) and the integral will therefore restrict the l -values to 0 and 2. A $J' = 7/2$ level will then not decay to the ground state, but can emit protons to the 2^+ (and 4^+) levels. The $J' = 3/2, 5/2$ levels can decay to the ground state by emitting a d-wave proton and to the 2^+ level by d- or s-wave, but s-wave is only allowed for $K' = 1/2$.

A. Proton emission results

An overview of the current experimental knowledge on the structure of ^{21}Na can be found through the papers [14, 16]. Parts of the pertinent information on the levels that appear in the decay are reproduced in Table I, and the observed proton spectrum from [14] is shown in Figure 4. The figure shows the singles proton spectrum and many excited levels could energetically decay both to the 0^+ ground state and 2^+ first excited state in ^{20}Ne ; for each level the position of the protons from these two transitions is marked, and Table I includes the observed branching ratios b_0 and b_2 of the two transitions as well as the penetrability for s- and/or d-wave emission for the transitions. For ease of reference, the most relevant parts of the decay scheme are reproduced also in Figure 3.

The penetrabilities are relevant for two different aspects: (1) in the wave function overlap integral the penetrability gives the approximate value of how much the continuum wave function is suppressed by the Coulomb and angular momentum barriers; (2) we may estimate the width of a level via R-matrix theory (see e.g. chapter 10 in [9]) as twice the penetrability times the reduced width, an upper limit of which is the so-called Wigner width, which here is about 1.6 MeV. The ratio of penetrabilities therefore enters in the ratio b_2/b_0 and levels with large width Γ must have high values both of the penetrability and the wave function amplitude. This may be relevant for the levels at 5.02 MeV, 6.47 MeV and 7.49 MeV.

Table I also gives the deduced quantum numbers appearing from the following analysis.

The first level in ^{21}Na to emit protons to the 2^+ state is at 5.02 MeV (orange in Figs 3 and 4). It has about the same branching ratio to the two states in ^{20}Ne which strongly suggests that it proceeds via s-wave emission to the 2^+ state. It must therefore have $K' = 1/2$. Since protons are emitted to the ground state, the spin cannot

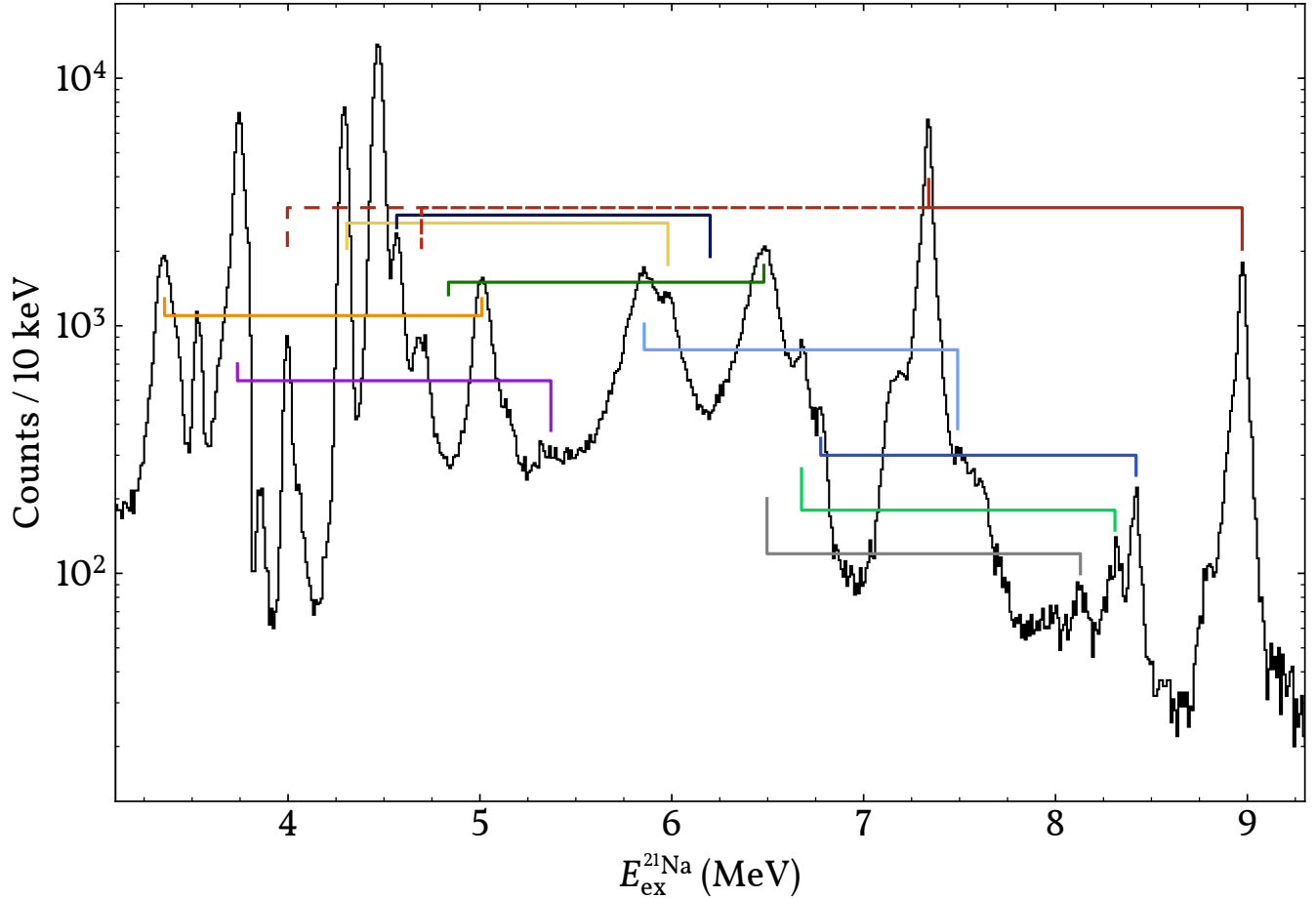


Figure 4: The beta-delayed proton spectrum recorded in [14] shown versus the excitation energy E_{ex} in ^{21}Na (deduced assuming the proton is emitted to the ^{20}Ne ground state). The solid lines connect peaks that originate from the same level, to the right the transition to the ground state, to the left to the excited 2^+ state in ^{20}Ne (displaced 1.634 MeV downwards). The IAS at 8.97 MeV decays also to higher excited states, this is indicated with the dashed line. Below $E_{ex} \approx 4.2$ MeV the shown intensities are displaced by factors 2–3, see [14] for details.

Table I: Beta-delayed protons from ^{21}Na . Results from the beta-decay experiment in [14] to the left, literature values from [16] in the middle, and penetrabilities and deduced J' and K' values to the right. E_{ex} is the excitation energy in ^{21}Na , Γ the level width and b_p the branching ratio.

E_{ex} (MeV)	b_p (%) ^a		$E_{ex}(\text{lit})$ (keV)	$\Gamma(\text{lit})$ (keV)	J'^{π}	Penetrability			J'	K'
	0^+	2^+				gs, $l = 2$	$2^+, l = 0$	$2^+, l = 2$		
5.02(1)	4.6(3)	4.4(4)		110(15) ^b		0.134	0.061	0.0016	$3/2, 5/2$	$1/2$
5.37(1)	< 0.4	10.8(4)				0.201	0.186	0.008	$7/2$	
5.98(2)	0.15(5)	< 0.05				0.344	0.488	0.044	$3/2^b$	$(3/2)$
6.20(1)		1.5(4)				0.402	0.603	0.068	$7/2$	
6.47(2)	6.5(6)	0.5(3)	6468(20)	145(15)	$3/2^+$	0.476	0.740	0.104		$3/2$
7.49(2)	< 1.4	7.2(6)	7609(15)	112(20)	$3/2^+$	0.777	1.203	0.313		$1/2$
8.13(2)	0.16(3)	0.5(3)	8135(15)	32(9)	$5/2^+$	0.970	1.453	0.484		
8.31(2)	0.20(2)	0.6(2)	8397(15)	30(13)	$3/2^+$	1.024	1.518	0.535		
8.42(2)	0.23(2)	0.4(2)	8464(15)	25(9)	$3/2^+$	1.057	1.557	0.567		
8.97(1)	2.10(3)	8.4(3)	8976(2)	0.65(5)	$5/2^+$	1.219	1.742	0.730		$1/2$

^aThe fraction of the total beta-delayed proton spectrum.

^bValue deduced in [14].

be $7/2$.

The next level at 5.37 MeV (purple) has a b_2 more than 20 times larger than b_0 , so the latter decay is strongly hindered. It must therefore have $J' = 7/2$, which is consistent with the assignment in [15]. In a similar way, the 6.20 MeV level (dark blue) is only observed to decay to the excited state, and must also have $J' = 7/2$.

The 5.98 MeV level (yellow) is assigned in [14] as $J' = 3/2$ and is only seen to decay to the ground state. The excited state transition would lie below one of the strongest proton peaks and is weaker by more than a factor 3, which could indicate that K' cannot be $1/2$; it must then be $3/2$. A similar argument applies for the 6.47 MeV level (dark green) that is known to have $J' = 3/2$ and has a b_0 more than an order of magnitude larger than b_2 . This indicates that both proton transitions occur with $l = 2$ and implies that the level has $K' = 3/2$.

The 7.49 MeV level (light blue) is also $J' = 3/2$, but decays mainly (by a factor more than 5) to the excited 2^+ state. That points to $K' = 1/2$ and a rather high s-wave content in its wave function. In the same way one can argue that the $J' = 5/2$ IAS at 8.97 MeV (red) has $K' = 1/2$, as is expected since it is the analogue of the ^{21}Mg ground state.

The three levels at 8–8.5 MeV (grey, light green and blue) are all observed to decay to both states in ^{20}Ne (consistent with their literature spin assignments), but the accuracy of their branching ratios is too low to give information on their K -values.

B. Structural implications

A suggested assignment of Nilsson single-particle configurations to the lowest bands in ^{21}Ne is given in Table 5-8 in [1] and should be very similar to the one of ^{21}Na . Assignments for K -values for both nuclei are given in [15] and differ mainly in the interpretation of the lowest $K' = 1/2$ band that is attributed to $[211]1/2$ in [1] and rather to a core excited configuration (e.g. $[220]1/2$) in [15], note that these two configurations could be expected to lie close in excitation energy and therefore could be susceptible to Coriolis mixing. Apart from this and the $[211]3/2$ ground state band, both sources attribute two negative parity bands to core excitations ($[101]1/2$ and $[330]1/2$). This exhausts the structure up to 4–5 MeV [15, 16].

The remaining single-particle configurations are $[202]5/2$, $[200]1/2$ (most likely with a small decoupling parameter) and $[202]3/2$. It is important to note that more complex configurations will come from exciting protons or neutrons from the $[220]1/2$ orbit (a clear example is the IAS that furthermore has a different isospin value), but these can not be described with our simplest model ansatz. The simplification in Eq.(12) no longer holds and we will now need to evaluate the more complex integral in Eq.(6), but the selection rules are still very similar. The proton decay of the levels is likely to be hindered

and the levels would naturally become narrow.

We do not expect sizable beta-decay to the $[202]5/2$ configuration due to the K -difference of 2. This is at variance with the interpretation in [15] of the $5/2^+$ level at 4294 keV and the $7/2^+$ level at 5.37 MeV as belonging to a $K' = 5/2$ band. We would rather expect them to be related in a $K' = 3/2$ band.

Using the estimated energies of the configurations from [15] one could expect the $[202]3/2$ configuration to correspond to the $K' = 3/2$ band that starts at the 6.47 MeV level, and the $[200]1/2$ configuration to start slightly lower in energy (but note that it may mix with the other $K' = 1/2$ bands). The wide 5.02 MeV level is more likely to be a member of the $[211]1/2$ band, but the 7.49 MeV level could belong to the $[200]1/2$ band that has a relatively large s-wave component cf. Table 5-9 in [1]. A large level width is due to either s- or d-wave strength.

The IAS in itself cannot proton decay due to isospin conservation, but it is likely to mix with two other close-lying levels [14]. One of these is rather broad and may be related to the 7.49 MeV level, this would then facilitate the proton decays to the ground state band in ^{20}Ne . The decays to the 2^- band (transitions are known to both the 2^- and 3^- levels) may then be due to mixing with the other level. Comparing the branching ratios and penetrabilities to the different final states [14] one observes a structural preference for decays to the 2^- and 4^+ states. As a potential signature, we note that the broad component around the IAS seems present in the 4^+ gated spectrum, but not in the 2^- gated spectrum in [14]. More statistics would be needed to resolve this.

We note that the simple particle-rotor picture for the beta decay lets the $1/2^+$ state in the intrinsic frame go to either $1/2^+$ or $3/2^+$ (these then become the K' -values) to which the core rotation must be added. The $3/2^+$ ground state in a $K' = 3/2$ band may therefore be hindered in beta feeding compared to the $5/2^+$, $7/2^+$ members, which fits with the skew beta feeding pattern observed to the ground state band (Table 3 in [14]).

The preference for proton emission to the final 2^+ rotational state seems related to the fact that the initial state has a core in a 2^+ rotation. The beta decay will preferentially go to ^{21}Na states that overlap with the rather simple structure of the Gamow-Teller Giant Resonance (GTGR, a spin- and isospin-flip of the ^{21}Mg ground state). The proton emission of these states select components with composition one proton plus a ^{20}Ne state; as the GTGR lies at a somewhat high energy, many components of the states fed in the beta decay can be expected to have a rather complex structure, so it is not that surprising if the simple rotational component fed in beta decay overlaps with the simple rotational component preferred in the proton emission.

C. Emission of α -particles

In the case of ^{21}Na the final state after emission of an α -particle is ^{17}F , which is not deformed. The formalism will therefore not apply, but the main physics ingredients in the particle emission will be the conservation of angular momentum and an overlap matrix element, so the difference to the deformed case mainly lies in the Clebsch-Gordan coefficient with the K quantum number. The observed α -decays stem from levels around the IAS, which as discussed above have a more complex structure.

D. Particle emission from other sd-shell nuclei

As mentioned briefly earlier, the beta-decay selection rule on K has been demonstrated in charge-exchange reactions on ^{23}Na and ^{25}Mg [8], but is of course also well known from heavier nuclei [1].

The derived formalism is directly applicable to the beta decay of odd mass nuclei where the beta daughter through nucleon emission goes to an even-even nucleus. The beta-delayed proton emission from ^{21}Mg is therefore expected to be similar to the one from the nuclei $^{23,25}\text{Si}$ and $^{27,29}\text{S}$.

For beta-delayed neutron emission the formalism is suited for initial nuclei with odd Z and even N , such as ^{29}Na .

For beta-delayed α -particle emission other cases are the nuclei ^{20}Na and ^{22}Al .

It could be interesting to expand the treatment to decays to odd nuclei/odd-odd nuclei in the sd-shell, such as the decays of ^{22}Al , ^{24}Si and ^{26}P . There is as yet little relevant data available in higher mass regions.

VII. SUMMARY AND CONCLUSIONS

Rotational bands in deformed nuclei are typically identified and studied through the internal gamma transitions in the band. As the excitation energy in a nucleus increases, particle emission will eventually dominate over gamma emission and other probes of rotational structure must be used. This paper was motivated by a study of beta-delayed particle emission in the lower sd-shell, i.e. in relatively light nuclei away from the line of beta-stability where the level density at excitation energies of 5–10 MeV is not too high, and level widths are in the keV range and already dominated by particle decays. These states may also be populated in particle elastic scattering or transfer reactions, but the selection rules of the beta decay process will give a sparse feeding and give clean results.

Our derivation resulted in selection rules, in particular for the K quantum number, and the finding that structural overlap is important for the pattern of particle emissions. These results were illustrated through data from the beta decay of ^{21}Mg and yielded an interpretation of the feeding of levels in ^{21}Na ; the analysis presented here

is helpful in understanding the structure of the particle emission pattern as well as in assigning J and K values to the levels. Rotational structure have in this way been identified in ^{21}Na up to the 5–10 MeV energy range. We note that the fact that ^{21}Mg has spin-parity $5/2^+$, but only $K = 1/2$, gives more structure information from the decay.

The simplest results depended on the assumption that it is the same core rotating throughout the decay. If this is not the case, the Clebsch-Gordan selection rules will be the same, but the overlap integral (giving the “fingerprint” interpretation in the related case of transfer reactions) will have a higher dimensionality and invoke the coordinates of more particles and the interpretation correspondingly becomes more complex. In slightly more detail, our simple result hinges on the approximation that the structure of the initial and final state is the same apart from the extra particle that is emitted. In essence, it should apply when structure development is gradual.

Apart from the clear link between beta-delayed particle emission and transfer experiments, there is also a close correspondance to the outgoing step in (in)elastic scattering experiments. Much of our analysis of how the decay pattern from an excited level can be used to extract structure information can of course be taken over (we did not find such information in the $p+^{20}\text{Ne}$ case). Our results for beta-delayed proton emission could in part be applied also to proton radioactivity from deformed nuclei where, however, more accurate and detailed approaches have been employed, e.g. for the decay of ^{131}Eu in [17].

In conclusion, beta-delayed particle decays just a few steps away from the line of beta-stability can, via the particle emission process, give access to spectroscopic information that complements and extends what is achievable via classical reaction experiments. Transfer reactions are of course now also possible with radioactive beams, but will typically require significantly larger intensities than beta-decay experiments. Our results will be straightforward to extend and apply to higher mass regions.

Acknowledgments

This work has been partially supported by the Independent Research Fund Denmark (9040-00076B). We wish to acknowledge several illuminating discussions with Thomas Døssing.

Appendix A: Rotations: Definitions and Properties

The notation and definitions are originally from [1], and following [2] for completeness reformulated to be directly applicable in the present connection in [3].

The rotation operator, $\mathcal{R}_{\vec{\omega}}$ is defined by

$$\mathcal{R}_{\vec{\omega}} = \exp(-i\phi J_z) \exp(-i\theta J_y) \exp(-i\psi J_z). \quad (\text{A1})$$

in terms of the three Euler angles, $\vec{\omega} = (\phi, \theta, \psi)$, and the components of the angular momentum operator, $\vec{J} = (J_x, J_y, J_z)$. This operator describes a general rotation from one given direction to another. Any coordinate, \mathbf{r}_i , is then transformed into $\mathbf{r}'_i = \mathcal{R}_{\vec{\omega}} \mathbf{r}_i$.

The convenient basis is $|JM\rangle$, that is the eigenstates of J^2 and J_z . The matrix elements of $\mathcal{R}_{\vec{\omega}}$ define the D -functions

$$\langle JM | \mathcal{R}_{\vec{\omega}} | J'M' \rangle = \delta_{J,J'} \mathcal{D}_{MM'}^{J*}(\vec{\omega}). \quad (\text{A2})$$

The angles, (θ, ϕ) , are precisely defined as the angles in the spherical harmonics, $Y_{lm}(\theta, \phi)$, and ψ is the angle describing rotation about the z -axis of the possibly extended system. The relation is

$$\mathcal{D}_{M0}^J(\vec{\omega}) = \sqrt{4\pi/(2J+1)} Y_{JM}(\theta, \phi), \quad (\text{A3})$$

and the orthonormality conditions are

$$\int d^3\vec{\omega} \mathcal{D}_{MK}^{J*}(\vec{\omega}) \mathcal{D}_{M'K'}^J(\vec{\omega}) \equiv \int_0^\pi \sin\theta d\theta \int_0^{2\pi} d\phi \quad (\text{A4})$$

$$\int_0^{2\pi} d\psi \mathcal{D}_{MK}^{J*}(\vec{\omega}) \mathcal{D}_{M'K'}^J(\vec{\omega}) = \frac{8\pi^2}{2J+1} \delta_{JJ'} \delta_{MM'} \delta_{KK'}.$$

Successive rotations of the same angles can be collected into one, that is

$$\mathcal{D}_{M_1K_1}^{J_1}(\vec{\omega}) \mathcal{D}_{M_2K_2}^{J_2}(\vec{\omega}) = \sum_{J=|J_1-J_2|}^{J_1+J_2} \mathcal{D}_{M_1+M_2, K_1+K_2}^J(\vec{\omega})$$

$$\langle J_1 M_1 J_2 M_2 | J, M_1 + M_2 \rangle \langle J_1 K_1 J_2 K_2 | J, K_1 + K_2 \rangle (\text{A5})$$

Combining successive different rotations

$$\mathcal{R}_{\vec{\omega}} = \mathcal{R}_{\vec{\omega}'} \mathcal{R}_{\vec{\omega}''} \quad (\text{A6})$$

$$\mathcal{R}_{\vec{\omega}}^{-1} = \mathcal{R}_{-\vec{\omega}} = \mathcal{R}_{-\vec{\omega}'} \mathcal{R}_{-\vec{\omega}''}$$

leads to corresponding relations between the D -functions

$$\mathcal{D}_{MK}^{J*}(\vec{\omega}) = (-1)^{M-K} \mathcal{D}_{-M-K}^J(-\vec{\omega})$$

$$= (-1)^{M-K} \sum_L \mathcal{D}_{-M-L}^J(-\vec{\omega}') \mathcal{D}_{-L-K}^J(-\vec{\omega}'') \quad (\text{A7})$$

$$= \sum_L \mathcal{D}_{ML}^{J*}(\vec{\omega}') \mathcal{D}_{LK}^{J*}(\vec{\omega}'').$$

The effects on the coordinates are

$$\mathbf{r}'_i = \mathcal{R}_{\vec{\omega}} \mathbf{r}_i \quad (\text{A8})$$

$$\mathcal{R}_{\vec{\omega}} \mathbf{r}_i = \mathcal{R}_{\vec{\omega}} \mathcal{R}_{\vec{\omega}'}^{-1} \mathbf{r}'_i \equiv \mathcal{R}_{\vec{\omega}'} \mathbf{r}'_i.$$

Transformation of a coordinate (or spin dependent) tensor, $T_{\lambda\mu}(\mathbf{r}_i)$, of rank λ is

$$T_{\lambda\mu}(\mathbf{r}_i) = T_{\lambda\mu}(\mathcal{R}_{\vec{\omega}}^{-1} \mathbf{r}'_i) = \sum_{\mu'} \mathcal{D}_{\mu\mu'}^\lambda(\vec{\omega}') T_{\lambda\mu'}(\mathbf{r}'_i) \quad (\text{A9})$$

Finally, we shall need the following

$$\int d^3\vec{\omega} \mathcal{D}_{mm'}^{j*}(\vec{\omega}) \mathcal{D}_{ML}^{J*}(\vec{\omega}) \mathcal{D}_{M'K'}^J(\vec{\omega})$$

$$= \frac{8\pi^2}{2J'+1} \langle JMjm | J'M' \rangle \langle JLjm' | J'K' \rangle. \quad (\text{A10})$$

Appendix B: The internal wavefunction

Depending on the symmetries of the internal wavefunction, the statements in section II may have to be modified. We shall assume here that axial symmetry is present. Consider first the case of a nucleus with intrinsic spin 0^+ and $K = 0$ in a rotational state J (we also assume positive parity for the intrinsic wavefunction). Following the derivation in [3], the normalization integral in section II.C will then apart from the contribution around $\theta = 0$ also get a contribution around $\theta = \pi$ which will have the same value as at $\theta = 0$, but with a phase factor $(-1)^J$. This doubles the value of the integral for even J and shows the well-known result that odd J do not occur. Other axially symmetric cases will also go from one to two contributions, but the phase factor will become $(-1)^{J+K}$ as shown in [1] chapter 4-2 and appendix 4A and for a non-zero value of K the projection on the internal axis of course changes sign for the contributions at $\theta = \pi$. The case of odd A (a fermion) is slightly more complex and one must use instead the time-reversed wavefunction $\varphi_{K'} = -\varphi_{-K'}$.

These results must be inserted in Eq.(13). The change in the overlap integral $ME/\sqrt{N_i N_f}$ will be a doubling to two terms (the second term with the above combined phase factor) and the change in normalization will simply be a factor $1/\sqrt{2}$. The expression therefore becomes

$$\frac{ME}{\sqrt{N_i N_f}} = 4\pi \sqrt{\frac{2J+1}{2(2J'+1)}} \sum_{j,l,m_l,m'_l,\Sigma'_p} (-i)^l Y_{l,m_l}(\hat{\mathbf{k}}_p)$$

$$\langle JMjm_l + \Sigma_p | J'M' \rangle \langle lm_l s \Sigma_p | jm_l + \Sigma_p \rangle$$

$$[\langle JKjm'_l + \Sigma'_p | J'K' \rangle \langle lm'_l s \Sigma'_p | jm'_l + \Sigma'_p \rangle$$

$$\int d^3\mathbf{r}_p \chi_{\Sigma'_p}^\dagger j_l^*(k_p r_p) Y_{l,m'_l}^*(\hat{\mathbf{r}}_p) \varphi_{K'}(\mathbf{r}_p) - \quad (\text{B1})$$

$$(-1)^{J'+K'} \langle JKjm'_l + \Sigma'_p | J' - K' \rangle \langle lm'_l s \Sigma'_p | jm'_l + \Sigma'_p \rangle$$

$$\int d^3\mathbf{r}_p \chi_{\Sigma'_p}^\dagger j_l^*(k_p r_p) Y_{l,m'_l}^*(\hat{\mathbf{r}}_p) \varphi_{-K'}(\mathbf{r}_p)].$$

We can now in the second term change the signs of the sum indices for m'_l and Σ'_p and use that $\langle j_1 - m_1 j_2 - m_2 | j_3 - m_3 \rangle = (-1)^{j_1+j_2-j_3} \langle j_1 m_1 j_2 m_2 | j_3 m_3 \rangle$ to simplify the expression for $K = 0$ to

$$\frac{ME}{\sqrt{N_i N_f}} = 4\pi \sqrt{\frac{2J+1}{2(2J'+1)}} \sum_{j,l,m_l,m'_l,\Sigma'_p} (-i)^l Y_{l,m_l}(\hat{\mathbf{k}}_p)$$

$$\langle JMjm_l + \Sigma_p | J'M' \rangle \langle lm_l s \Sigma_p | jm_l + \Sigma_p \rangle$$

$$\langle J0jm'_l + \Sigma'_p | J'K' \rangle \langle lm'_l s \Sigma'_p | jm'_l + \Sigma'_p \rangle$$

$$\left[\int d^3\mathbf{r}_p \chi_{\Sigma'_p}^\dagger j_l^*(k_p r_p) Y_{l,m'_l}^*(\hat{\mathbf{r}}_p) \varphi_{K'}(\mathbf{r}_p) + \quad (\text{B2})$$

$$(-1)^\Xi \int d^3\mathbf{r}_p \chi_{-\Sigma'_p}^\dagger j_l^*(k_p r_p) Y_{l,-m'_l}^*(\hat{\mathbf{r}}_p) \varphi_{-K'}(\mathbf{r}_p) \right],$$

where the final total phase factor becomes $\Xi = -1 + J' + K' + (J + j - J') + (l + s - j) = J + K' + l + s - 1$.

For the case in section III with $K' = 1/2$, $s = 1/2$ and $l = 0$ we end up with a phase factor $(-1)^J$ and the two terms therefore give the same contribution for J even. Inserting also the numerical value of the last Clebsch-Gordan coefficient that for $K = 0$ is $\sqrt{1/2}\sqrt{(2J'+1)/(2J+1)}$ reduces the final result to

$$\frac{ME}{\sqrt{N_i N_f}} = \sqrt{4\pi} \langle JM \frac{1}{2} \Sigma_p | J' M' \rangle$$

i.e. the same as Eq.(20), as expected.

$$\int d^3 \mathbf{r}_p J_0^*(k_p r_p) \varphi_{K'}(r_p), \quad (\text{B3})$$

-
- [1] A. Bohr and B.R. Mottelson, Nuclear Structure, Vol 1 and 2, Benjamin, Reading Massachusetts, 1969, 1975.
- [2] F. Villars, Many-Body Description of Nuclear Structure and Reactions, Proc. Int. School of Physics, Enrico Fermi 36, (1966) 14.
- [3] P.J. Siemens and A.S. Jensen, Elements of Nuclei, Many-body Physics with the Strong Interaction, Chapter 9, Addison-Wesley Publishing Company, California, 1987.
- [4] Nuclear Decay Modes, ed. D.N. Poenaru (Institute of Physics, Bristol, 1996).
- [5] M. Pfützner, M. Karny, L.V. Grigorenko, K. Riisager, Rev. Mod. Phys. 84 (2012) 567.
- [6] B. Jonson and K. Riisager, Nucl. Phys. A 693, 77 (2001).
- [7] G. Alaga, Nucl. Phys. 4, 625 (1957).
- [8] Y. Fujita, B. Rubio, W. Gelletly, Prog. Part. Nucl. Phys. 66, 549 (2011).
- [9] I.J. Thompson and F.M. Nunes, Nuclear Reactions for Astrophysics, (Cambridge University Press, 2009).
- [10] B. Elbek and P.O. Tjøm, Advances in Nuclear Physics, vol. 3, eds. M. Baranger and E. Vogt (Plenum Press, New York, 1969) p. 259
- [11] J.P. Elliott and C.E. Wilsdon, Proc. Roy. Soc. A 302, 509 (1968).
- [12] M. Kimura and N. Furutachi, Phys. Rev. C 83, 044304 (2011).
- [13] Z.H. Sun, T.R. Djärv, G. Hagen, G.R. Jansen, T. Papenbrock, arXiv:2409.02279
- [14] E.A.M. Jensen et al., Eur. Phys. J. A (2024) 60:153.
- [15] R. Bijker and F. Iachello, Nucl. Phys. A 1010 (2021) 122193.
- [16] R.B. Firestone, Nuclear Data Sheets 127 (2015) 1.
- [17] A.T. Kruppa, B. Barmore, W. Nazarewicz and T. Vertse, Phys. Rev. Lett. 84 (2000) 4549.